OXFORD

ORIGINAL ARTICLE

Overexpression of *KLC2* due to a homozygous deletion in the non-coding region causes SPOAN syndrome

Uirá S. Melo[1,†], Lucia I. Macedo-Souza[1,†], Thalita Figueiredo[2,3], Alysson R. Muotri[4], Joseph G. Gleeson[5], Gabriela Coux[6], Pablo Armas[6], Nora B. Calcaterra[6], João P. Kitajima[7], Simone Amorim[8], Thiago R. Olávio[1], Karina Griesi-Oliveira[1], Giuliana C. Coatti[1], Clarissa R.R. Rocha[9], Marinalva Martins-Pinheiro[9], Carlos F.M. Menck[9], Maha S. Zaki[10], Fernando Kok[1,7], Mayana Zatz[1,*] and Silvana Santos[2,3]

[1]Human Genome and Stem Cell Research Center, Department of Genetics and Evolutionary Biology, Biosciences Institute, University of Sao Paulo (USP), Sao Paulo, SP 05508-090, Brazil, [2]Northeast Biotechnology Network (RENORBIO), Federal University of Paraiba (UFPB), Joao Pessoa, PB 58051-900, Brazil, [3]Department of Biology, Paraiba State University (UEPB), Campina Grande, PB 58429-500, Brazil, [4]Department of Pediatrics/Rady Children's Hospital San Diego, University of California San Diego, La Jolla, CA 92093, USA, [5]Laboratory for Pediatric Brain Disease, The Rockefeller University, New York, NY 10065, USA, [6]Instituto de Biología Molecular y Celular de Rosario (IBR), Consejo Nacional de Investigaciones Científicas y Técnicas (CONICET) – Facultad de Ciencias Bioquímicas y Farmacéuticas, Universidad Nacional de Rosario (UNR), Rosario, SF S2002LRK, Argentina, [7]Mendelics Genomic Analysis, São Paulo, SP 04013-000, Brazil, [8]Department of Neurology, School of Medicine, University of Sao Paulo (USP), São Paulo, SP 01246-903, Brazil, [9]Department of Microbiology, Institute of Biomedical Sciences, University of São Paulo (USP), São Paulo, SP 05508-900, Brazil and [10]Department of Clinical Genetics, Human Genetics and Genome Research Division, National Research Center, Cairo 12311, Egypt

*To whom correspondence should be addressed at: Rua do Matao, 277, Cidade Universitária, São Paulo, SP CEP 05508-900, Brazil. Tel: +55 1130917563; Fax: +55 1130917419; Email: mayazatz@usp.br

Abstract

SPOAN syndrome is a neurodegenerative disorder mainly characterized by spastic paraplegia, optic atrophy and neuropathy (SPOAN). Affected patients are wheelchair bound after 15 years old, with progressive joint contractures and spine deformities. SPOAN patients also have sub normal vision secondary to apparently non-progressive congenital optic atrophy. A potential causative gene was mapped at 11q13 ten years ago. Here we performed next-generation sequencing in SPOAN-derived samples. While whole-exome sequencing failed to identify the causative mutation, whole-genome sequencing allowed to detect a homozygous 216-bp deletion (chr11.hg19:g.66,024,557_66,024,773del) located at the non-coding upstream region of the *KLC2* gene. Expression assays performed with patient's fibroblasts and motor neurons derived from SPOAN patients showed *KLC2* overexpression. Luciferase assay in constructs with 216-bp deletion confirmed the overexpression of gene reporter, varying from 48 to 74%, as compared with wild-type. Knockdown and overexpression of *klc2* in *Danio rerio* revealed mild to severe

6877

curly-tail phenotype, which is suggestive of a neuromuscular disorder. Overexpression of a gene caused by a small deletion in the non-coding region is a novel mechanism, which to the best of our knowledge, was never reported before in a recessive condition. Although the molecular mechanism of *KLC2* up-regulation still remains to be uncovered, such example adds to the importance of non-coding regions in human pathology.

Introduction

Hereditary spastic paraplegias (HSPs) are common neurodegenerative genetic disorders in which patients present progressive spasticity and lower limbs weakness. Up to date, more than 70 loci had been associated with HSPs and at least 50 genes have been identified (1). In 2005, our group identified in a geographic isolate in the backlands of Northeastern Brazil, 26 Caucasian individuals belonging to consanguineous families with an autosomal recessive (AR) complicated form of HSP, which associates spastic paraplegia, optic atrophy and neuropathy (SPOAN syndrome, OMIM #609541) (2). This condition is characterized by onset of progressive spastic paraplegia in infancy, and progressive motor and sensory axonal neuropathy in late childhood/early adolescence leading to severe motor disability. All patients are wheelchair bound after 15 years old, with progressive joint contractures and spine deformities. Patients also have sub normal vision secondary to apparently non-progressive congenital optic atrophy, dysarthria starting in the third decade of life and exacerbated acoustic startle response. Patients show no intellectual impairment. Ten years after the gene mapping, more than 70 individuals from this cluster, three unrelated affected individuals from Southern and Southeast Brazil, and a pair of Egyptian siblings were diagnosed with SPOAN. Although, all patients share the same haplotype spanning 2.3 Mb into chromosome region 11q13, Sanger sequencing of candidate genes failed to reveal the causative gene (3). Here we describe the SPOAN causative mutation, a small deletion in the non-coding region that causes gene overexpression. Gain of function in a recessive condition is a novel mechanism that, to the best of our knowledge, was never reported before.

Results

Next-generation sequencing and SPOAN mutation

Whole-exome sequencing (WES) was performed in genomic DNA from one Brazilian and one Egyptian patient diagnosed with SPOAN syndrome. We identified six homozygous variants at the critical region, but population frequency and segregation analysis excluded four variants, while the remaining two were SNPs located in non-coding region, suggesting that these two were unlikely to be associated to the clinical phenotype (Supplementary Material, Table S1). Although WES failed to reveal the SPOAN mutation, the sequencing allowed us to refine the critical interval on chromosome 11q13 to 1.77 Mb, between markers rs508548 (A>G at 65,626,289 position in *CFL1*) and an undescribed variant located at 67,395,410 (G>C in *NUDT8*). Next, using whole-genome sequencing (WGS), we identified a homozygous 216-bp deletion (chr11.hg19:g.66,024,557_66,024,773del), located at the non-coding upstream region of kinesin light chain-2 (*KLC2*) (Supplementary Material, Fig. S1). This variant was detected in homozygosity in all affected Brazilian individuals (*n* = 73), and in the Egyptian affected siblings, while it was not present in homozygosity in 111 healthy Brazilian relatives. This 216-bp deletion was also absent in 474 Brazilian healthy controls and is not described in the 1000 genomes database.

Gene expression analysis

To verify if the deletion affects the expression level of genes located in SPOAN critical region, we performed expression array using cDNA from fibroblasts. Several genes (*n* = 23; Supplementary Material, Table S2) showed differential expression in patients compared with controls (*P* < 0.01). Unexpectedly, this assay revealed *KLC2* overexpression. Quantitative reverse transcription PCR (RT-qPCR) performed using fibroblast cDNA samples confirmed the expression array results (Fig. 1A). We next generated induced pluripotent stem-cells (iPSC) which were differentiated into motor neurons (MN). RT-qPCR using MN samples revealed *KLC2* up-regulation in SPOAN patients compared with healthy controls, confirming the over expression observed in the previous experiments (Fig. 1C). Also we investigated *KLC2* expression in blood, using a larger number of cDNA samples from healthy controls, heterozygotes and affected individuals. This assay did not reveal any difference in expression levels between heterozygotes compared with SPOAN's and to healthy controls (Fig. 1E).

To investigate if the 216-bp deletion is the cause of *KLC2* up-regulation, we performed luciferase gene reporter assay using three cell lines (HEK293T, U87MG and MN), which were transfected with two constructs: a *KLC2* wild-type promoter and *KLC2* 216-bp deleted regulatory region driving the *Luciferase* gene. In the three cell lines, the construct with the 216-bp deletion produced a luciferase activity increment compared with wild-type promoter, varying from 48 to 74% (Fig. 1F).

Klc2 knockdown and overexpression in *Danio rerio*

We then used *Danio rerio* as an animal model to study the 'in vivo' effect of *klc2* knockdown and overexpression. Knockdown regulation was achieved by microinjecting zebrafish embryos with two different *klc2* morpholinos (translation blocking morpholino [MO$^{klc2\text{-}TB}$] and splice morpholino [MO$^{klc2\text{-}SP}$]), each one at doses of 4 and 6 ng. Mild phenotype was defined for embryos showing curly-tail and circular swimming whereas severe phenotype for embryos with dramatically shortened and twisted tail and that were unable to swim. Both phenotypes became evident at 48-h post fertilization (hpf) (Fig. 2A). In all cases, statistically significant differences were observed between mismatch-MO and specific-MO injected embryos. For both morpholino strategies when comparing to the respective mismatch-MO controls, an increase in lethality and/or frequency of phenotypes was mainly observed in detriment of normal phenotype. Furthermore, this difference was more evident when higher amount of either MO$^{klc2\text{-}TB}$ or MO$^{klc2\text{-}SP}$ was injected (Fig. 2B). Phenotype rescue assays were performed by co-injection of 100 pg of mRNA$^{klc2\text{-}eGFP}$ and splice morpholino at 6 ng (Fig. 2C), and an improvement of ~33% (*P* < 0.01), from severe to mild phenotype, was consistently observed (Fig. 2D).

As SPOAN syndrome seems to result from *KLC2* up-regulation, we mimicked this condition in zebrafish by microinjecting mRNA$^{klc2\text{-}eGFP}$ in specific concentrations in embryos. Fluorescent embryos displayed similar phenotype to *klc2* morphants (Fig. 3A). A high lethality (over than 70%) was observed in embryos microinjected with mRNA$^{klc2\text{-}eGFP}$ at 200 pg at 24-hpf stage and we excluded this concentration data in phenotype analysis (Fig. 3B). We observed higher frequency of curly-tail phenotype in
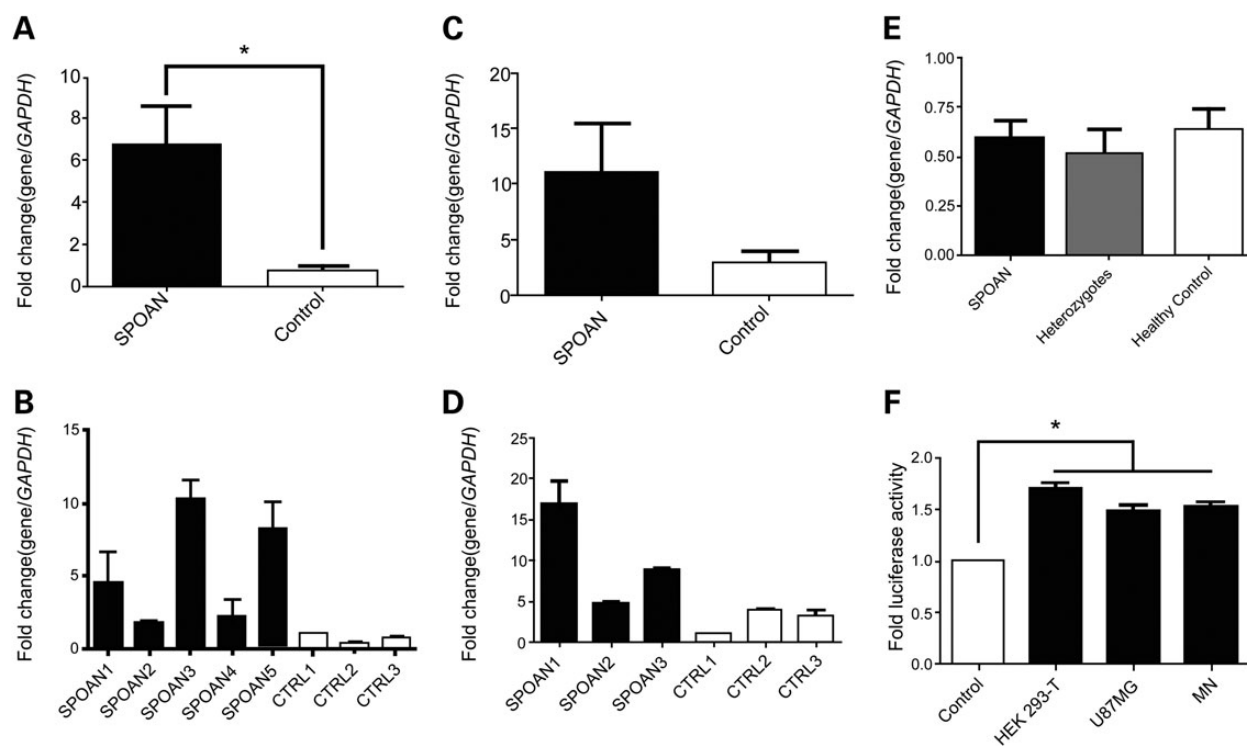
Figure 1. Effect of 216-bp deletion on *KLC2* expression. (**A**) Relative expression of *KLC2* measured by RT-qPCR performed on fibroblast cDNA isolated from SPOAN patients and healthy controls ($P < 0.05$; Nonparametric test [Mann–Whitney]). (**B**) *KLC2* relative expression measured on fibroflast samples from individual patients and healthy controls. (**C**) Relative expression of *KLC2* measured by RT-qPCR using MN. (**D**) *KLC2* relative expression measured on MN samples from individual patients and healthy controls. (**E**) *KLC2* relative expression measured on whole-blood cDNA samples from affected (homozygotes), heterozygotes and healthy controls. Each RT-qPCR experiment was performed in triplicate and each sample was replicated twice. (**F**) Expression of luciferase reporter gene controlled by the 216-bp-deleted *KLC2* regulatory region relative to the expression controlled by the wild-type *KLC2* regulatory region measured in HEK293 T, U87MG and MN cells. Each experiment was performed in triplicate and each cell type was replicated twice ($P < 0.05$; One-way ANOVA).

embryos microinjected with mRNA$^{klc2-eGFP}$ compared with control (mRNA^{eGFP}), being statistical significant in embryos microinjected at 150 pg mRNA concentration ($P < 0.05$) (Fig. 3C).

Discussion

We previously mapped the SPOAN gene, responsible for a syndromic form of AR spastic paraplegia, at 11q13 (2,3). Based on next-generation sequencing, we were able to uncover a new causative mechanism for this condition. We observed that a small deletion in *KLC2* non-coding region is responsible for the gene up-regulation and SPOAN phenotype. Additionally, *BSCL2* and *FLRT1*, two genes previously associated with HSP and located nearby but outside the 11q13 critical region, were excluded as candidates (4,5). The Egyptian patients reported in this study as SPOAN carried the c.T2023C (stop loss) homozygous mutation in *FLRT1*, and were previously assigned by Novarino *et al.* (5) (Family 709) as SPG68. However, here we suggest that 216-bp deletion, shared by all SPOAN patients, is probably the causative mutation in both Egyptian siblings, rather than the reported *FLRT1* mutation.

KLC2 codes for KLC2, a protein involved in anterograde axoplasmatic transport of organelles and macromolecules cargoes (6–10). KLC2 is a part of kinesin protein-1 complex (11), which binds to kinesins heavy chain in a stoichiometric ratio of 1:1 (12), being highly expressed in neurons. Several neurodegenerative diseases show impairment in axonal transport (13,14) and some kinesins heavy chains (KIF5A, KIF1A and KIF1C) have been associated with HSP (15–18). Animal models have also shown

that disturbance of axonal transport proteins cause neurodegenerative disease and axon degeneration (10,19–21). Although the disease mechanism described here involves a homozygous deletion in a non-coding region, all these observations strongly suggest that *KCL2* is the causative gene for SPOAN.

According to the RepeatMask database, *KLC2* upstream region was generated by a non-LTR retrotransposon (L3/CR-1) insertion. DNA footprint and alignment of L3/CR-1 did not show conservation among distant species, but the high conservation observed among primates suggests it was inserted during the divergence of primates from other mammals. In several human populations, *KLC2* surrounding region (10-kb up- and downstream) and three described SNPs surrounding the mutation location have low fixation index (F_{ST}) (Supplementary Material, Fig. S2) (rs116801155, rs190099601 and rs76627914 with F_{ST} of 0.0044, 0.0002 and 0.0427, respectively), indicating a high conservation in humans.

Surprisingly, the small deletion in its non-coding upstream region causes *KLC2* overexpression, suggesting a novel molecular mechanism never report before, a gain of function in recessive condition. Intriguingly, the 216-bp deletion overlaps 9-bp of 5′-untranslated region (5′-UTR) of the largest *KLC2* transcript (NM_001134775.1), which means that this mutation is located at *KLC2* promoter region (upstream of the transcription start site [TSS]) and it should cause gene downregulation instead gain of function. Although this region has characteristics of a promoter (enrichment of H3Kme3, DNase I hypersensitive sites [DHS], RNA pol II binding sites, etc.), transcription factors complexes that bind at this region may act as transcriptional repressor, which could explain the gene up-regulation. Additionally, this
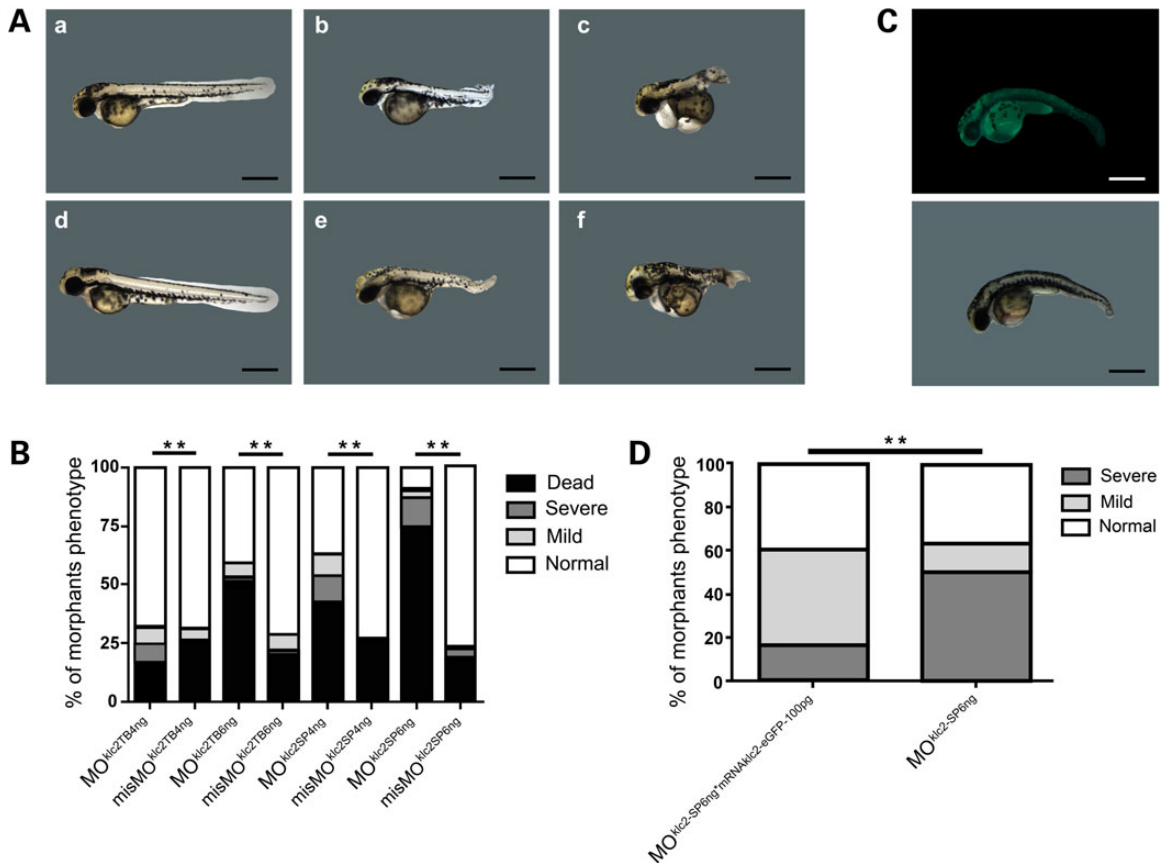
Figure 2. Effect of *klc2* knockdown in zebrafish. (**A**) (a and d) Embryos microinjected with control splicing blocking morpholino: (a) misMO$^{klc2\text{-}SP4ng}$ (d) misMO$^{klc2\text{-}SP6ng}$. (b, c, e and f) Embryos microinjected with splicing blocking morpholino: (b and c) MO$^{klc2\text{-}SP4ng}$ (e and f) MO$^{klc2\text{-}SP6ng}$. Normal (a and d), mild curly-tail (b and e) and severe curly-tail (c–f) phenotypes were recorded at 48-hpf. (**B**) Frequencies of observed phenotypes among morphants. Number of microinjected embryos: MO$^{klc2\text{-}TB4ng}$ (292); misMO$^{klc2\text{-}TB4ng}$ (305); MO$^{klc2\text{-}TB6ng}$ (103); misMO$^{klc2\text{-}TB6ng}$ (249); MO$^{klc2\text{-}SP4ng}$ (283); misMO$^{klc2\text{-}SP4ng}$ (234); MO$^{klc2\text{-}SP6ng}$ (423); misMO$^{klc2\text{-}SP6ng}$ (370). $P < 0.01$, χ^2 test. (**C**) Fluorescent embryo coinjected with 6 ng MO$^{klc2\text{-}SP}$ and 100 pg mRNA$^{klc2\text{-}eGFP}$ (selected by fluorescence at 24-hpf) showing mil-curly tails was recorded at 48-hpf. Scale bar 200 μm. (**D**) Embryos coinjected with 6 ng MO$^{klc2\text{-}SP}$ and 100 pg mRNA$^{klc2\text{-}eGFP}$ ($n = 70$ embryos) showed a partial rescue of morphant phenotype compared with MO$^{klc2\text{-}SP6ng}$ ($n = 30$ embryos). $P < 0.01$, χ^2 test.

deletion overlaps an unspliced antisense long non-coding RNA (lncRNA, AU311830.1) and regulatory elements: DHS, several transcription factors binding sites (TFBS), histone marks and DNA methylation (Supplementary Material, Fig. S1). Thus, a disruption of this non-coding and regulatory region might alter the expression level of downstream genes, which can explain SPOAN gain of function.

Expression analysis showed an unexpected *KLC2* overexpression from fibroblast and MN SPOAN samples. Because SPOAN is a recessive condition, we tried to check the *KLC2* expression pattern in heterozygous samples. Whole-blood samples collected from a large number of heterozygotes did not reveal increased *KLC2* expression, when compared with homozygotes and healthy controls. These results suggest a tissue-specific effect since 216-bp deletion causes *KLC2* up-regulation in fibroblast and MN cell-lines, but does not in blood. Also, luciferase assay showed that reporter constructs with 216-bp deletion have increased luciferase activity when compared with the wild-type. These results support the hypothesis that the 216-bp deletion located at non-coding region is likely the responsible for the *KLC2* overexpression.

Zebrafish has been an interesting animal model used in genetic studies due to its fast embryonic development and the fact it carries several human orthologues genes. The percentages of lethality and animals with curly-tail phenotype observed in morphants in this study were similar to those reported in several reports that employed zebrafish for other HSP (22–28). Microinjection of mRNA$^{klc2\text{-}eGFP}$ in zebrafish embryos showed a similar phenotype of *klc2* morphants, which reinforces our hypothesis that *klc2* is an essential gene for MN function and development. Thus, we hypothesize that imbalance of *KLC2* gene expression results in neurodegenerative phenotype in humans.

Gene overexpression had been associated with several neurological disorders but none of them have AR inheritance. For example, duplication or triplication of *PLP1* cause Pelizaeus-Merzbacher disease (OMIM #312080) (29–33) and *PMP22* duplication causes Charcot-Marie-Tooth disease type 1A (OMIM #118220), a hereditary demyelinating neuropathy (34,35). Variants detected upstream *APP* region were associated with up-regulation of APP protein in Alzheimer disease and Down syndrome patients (36). Additionally, downregulation or complete disruption of protein synthesis is usually the common mechanism in HSP in which functional studies have been conducted. For instance, this is the case in X-linked [e.g. *L1CAM* (37)], autosomal dominant [e.g. *ATL1* (38) and *SPAST* (39)] and AR conditions [as *SPG20* (40) and *FA2H* (41)].

In short, several unexpected and surprising results were observed during SPOAN syndrome molecular investigation. Although the molecular mechanism of this up-regulation still
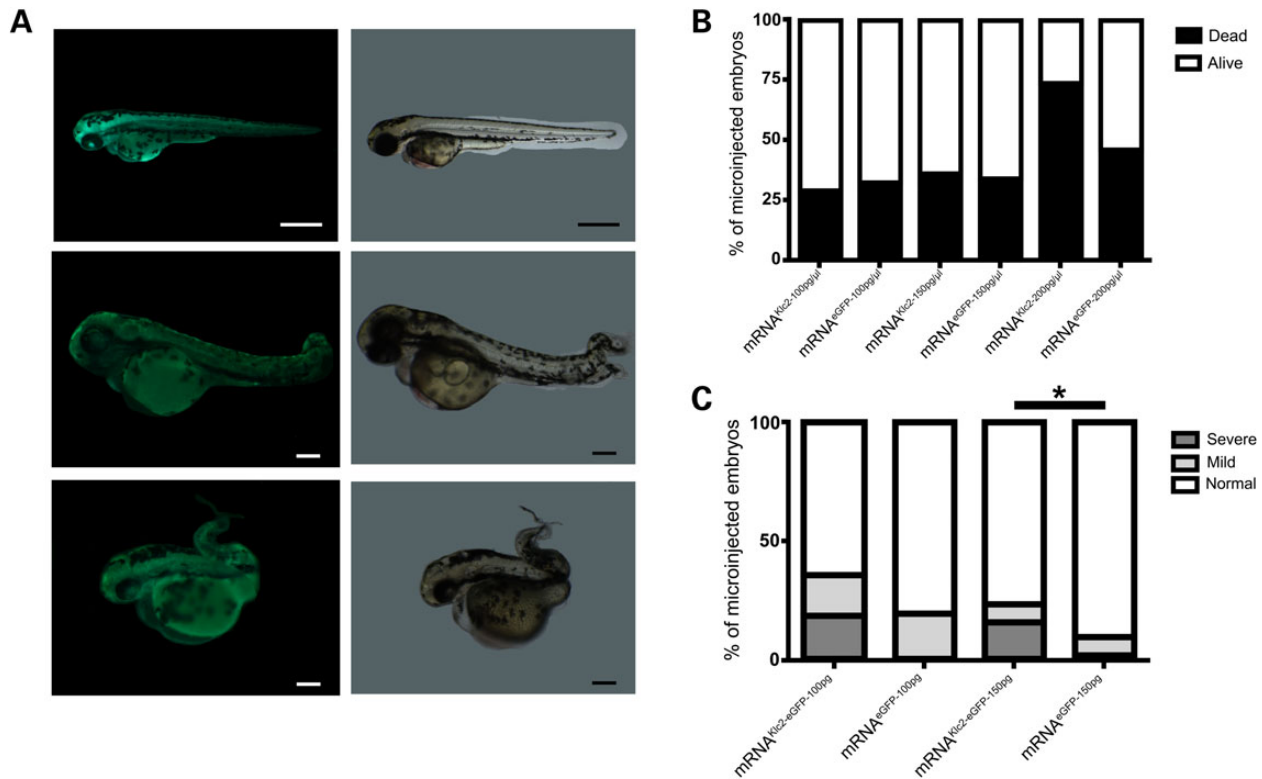
Figure 3. Effect of *klc2* overexpression in zebrafish. (**A**) (a and b) Embryos microinjected with 100 pg of mRNA^{eGFP} and (c–f) embryos microinjected with 100 pg of mRNA$^{klc2-eGFP}$ were selected by fluorescence at 24-hpf, and recorded at 48-hpf. (a and b) Normal Embryos, (c and d) mild curly-tail and (e and f) severe curly-tail phenotypes. Scale bars: (a and b) 200 µm; (c–f) 100 µm. (**B**) Lethality frequency observed in embryos at 24-hpf stage. Embryos microinjected with 200 pg mRNA$^{klc2-eGFP}$ showed high lethality and were excluded form phenotype analysis. (**C**) Frequencies of observed phenotypes among GFP-fluorescent embryos. Numbers of embryos selected by fluorescence: mRNA$^{klc2-eGFP-100pg}$ = 32; mRNA$^{eGFP-100pg}$ = 16; mRNA$^{klc2-eGFP-150pg}$ = 43; mRNA$^{klc2-eGFP-150pg}$ = 52. $P < 0.05$, χ^2 and Fisher's exact tests.

remains to be uncovered, it adds another example of the importance of non-coding regions in human pathology.

Materials and Methods

Patients

Clinical information regarding SPOAN patients in the geographic cluster detected in northeastern Brazil was detailed elsewhere (2,3). Additionally, we evaluated another three Brazilian patients, with different ancestors from northeastern Brazil and two Egyptians siblings with the identified 216-bp deletion and same clinical symptoms. Blood samples were used for DNA extraction from all patients, from several obligated carriers and from unaffected siblings. Fibroblasts were obtained from dermal biopsies from five patients, one heterozygote and four Brazilian healthy controls, following informed consent under protocols approved by the Biosciences Institute, University of São Paulo (Protocol CEP 010/2003).

Molecular analysis

Previous studies conducted by our group using Sanger sequencing did not identify deleterious variants in exons of candidates genes located in the critical region for SPOAN (*LRFN4*, *KLC2* and *CCS*) (3). To have a more comprehensive and detailed view over this region, WES was performed using DNA samples from two SPOAN subjects using Agilent SureSelect Human All Exon 50 Mb Kit and sequenced in Illumina HiSeq2000 (Illumina, San Diego, CA, USA). Alignment against reference GRCh37 was

performed with BWA (42); genotyping with GATK (43); SNP and InDel annotation with Annovar (44) and CNV detection with the R package ExomeDepth (45). The WES coverage achieved at the candidate region was 40× and 77× in the Egyptian and Brazilian samples, respectively. The 216-bp deletion was not detectable by WES. Variants detected in the mapped linkage region were filtered by their frequency, compared with 1000 Genomes database, NHLBI GO Exome Sequencing Project (ESP), Exome Aggregation Consortium (ExAC) and with sequences obtained from 1484 Brazilian controls.

Whole-genome sequencing was performed in DNA from a third affected patient (a distant cousin from Brazilian series) using Illumina TruSeq DNA kit. Alignment against reference GRCh37 was performed with BWA (42); genotyping with GATK (43); SNP and InDel annotation with SnpEff (46) and CNV detection using R package ExomeDepth (45) restricted to exon regions (using bedfile template of the Agilent V4Plus kit), Pindel and additional manual screening in the target linkage region. The achieved coverage at the candidate region was 26×. Variants were filtered by comparison with 1000 Genomes. SPOAN mutation (chr11.hg19:g.66,024,557_66,024,773del) was checked for co-segregation in affected and family health controls (also checked in 474 unrelated health controls) by PCR followed by agarose gel electrophoresis using primer ID 1 (Supplementary Material, Table S3).

Induced pluripotent stem-Cells (iPSC)

Retrovirus vectors containing the *Oct4*, *c-Myc*, *Klf4* and *Sox2* human cDNAs were obtained from Muotri's group and the

protocol is described elsewhere (47). Embryoid bodies (EBs) were formed by mechanical dissociation of cell clusters (pre-treated with dorsomorphin, 1 nM, for 2 days) and plating onto low-adherence dishes in NB media (DMEM/F12 plus 0.5X N2 and 0.5X B27 supplements) plus dorsomorphin for 2 days and in the next 5 days in NB media plus FGF and EGF. After that, mature EBs were dissociated with accutase for 5 min at 37°C and plated in matrigel in NB media plus FGF 20 ng/ml and EGF 20 ng/ml. Rosettes were visible for collection after 7 days and were then dissociated with accutase (Chemicon, EMD Millipore, Darmstadt, Germany) and plated onto poly-ornitine/laminin-coated dishes (Sigma) with NB media plus FGF and EGF. Homogeneous populations of neural progenitor cells (NPCs) were achieved after 1–2 passages with accutase in the same condition. To improve cell differentiation, brain-derived neurotrophic factor (20 ng/ml), glial cell-derived neurotrophic factor (20 ng/ml), insulin-like growth factor-1 (20 ng/ml), Ri (5uM) and SHH (100 ng/ml; neuronal maturation medium) were added to neuronal cultures for 5 weeks. NPCs were differentiated in MN following a protocol modified from study described elsewhere (48).

Human RNA extraction and cDNA synthesis

RNA extraction from fibroblasts ($n = 5$ affected; $n = 1$ heterozygote; $n = 4$ healthy controls) and MN ($n = 3$ affected; $n = 1$ heterozygote; $n = 3$ healthy controls) was performed with TRIZOL® reagent (Invitrogen) and Norgen Biotek RNA/DNA/Protein Purification Kit (Norgen Biotek Corp., Ontario, Canada); RNA from whole-blood ($n = 7$ affected; $n = 7$ heterozygotes; $n = 6$ family healthy controls +1 unrelated healthy control from the same region) were extracted using PAXgene Blood RNA Kit (Qiagen); RNA was reverse-transcribed with oligo(dT) primers using SuperScript™ III First-strand Synthesis System (Life Technologies).

Expression array

Fibroblast cDNA samples were submitted to array expression assay using GeneChip® Scanner 3000 7G System (Affymetrix, Santa Clara, CA, USA). The results of expression array were normalized by Robust Multi-array Average (49) and statistical method (test-T) was performed using CLCbio Genomics Workbench, adjusted by Bonferroni and false discovery rate (FDR). Data were submitted to GEO (accession number: GSE67527).

Quantitative reverse transcription PCR (RT-qPCR)

KLC2 primers for RT-qPCR were detailed in Supplementary Material, Table S3 (primer ID 2). RT-qPCR was normalized to *GAPDH* and was performed using LightCycler® 480 (Roche Diagnostics). *KLC2* expression data were calculated using $2^{-\Delta\Delta CT}$ method (50). Mann–Whitney test (Nonparametric) was performed using GraphPad Prism version 5.00 (San Diego, CA, USA). Each experiment was performed in triplicate and each sample was replicated twice.

TaqMan Gene Expression Assay probes: MNX1/HB9 (Hs00907365_m1), CHAT (Hs00252848_m1) and ISL1 (Hs00158126_m1) were used to validate the neurons derived cells from iPSC as MN (Applied Biosystems, USA). RT-qPCR was normalized to Human ACTB (β-actin; Hs01060665_g1). RT-qPCR was performed using the Applied Biosystems® 7500 Fast Real-time PCR System.

Immunofluorescence and MN validation

For immunofluorescence evaluation of MN, cells were fixed with 4% paraformaldehyde, followed by permeabilization and blocking with 0.05% (v/v) Triton X in PBS containing 5% (v/v) donkey serum. Primary antibodies were incubated overnight at 4°C. Samples were washed three times before secondary antibodies incubation (Alexa Fluor Dyes, Life Technologies). Dapi was added in the last 20 min of secondary antibody incubation. Primary antibody concentrations were: a-NeuN mouse monoclonal 1:500 (Millipore); a-Hb9 mouse polyclonal 1:500 (DSHB) and a-Islet 1 rabbit polyclonal 1:1000 (BD Bio-science). Images were obtained through Axio Observer.A1 immunofluorescence microscope (Zeiss). cDNA obtained from fibroblasts, NPC and MN were used for MN validation using TaqMan probes described above. RT-qPCR using fibroblast samples did not show expression of MN probes. RT-qPCR of MN samples showed expression of MNX1/HB9 probe, which was not amplified in NPC samples. MN samples showed higher significant ($P < 0.05$) expression of CHAT compared with NPC (Supplementary Material, Fig. S3B). We confirmed the presence of 216-bp deletion in DNA extracted from MN patient samples (Supplementary Material, Fig. S3C).

Gene reporter assay

The full-length (3,313-bp) and deleted 216-bp (3,097-bp) *KLC2* upstream region was synthesized (Genone) and cloned into promoterless firefly luciferase vector pGL4 (Promega). pShuttle/RL was used for transfection normalization, which expresses the reporter gene *Renilla* luciferase (51). Assays using HEK239T, U87MG and MN about 1×10^4 cells were plated in 96-well dishes in triplicate for each point. In HEK239T and U87MG a total of 200 ng of plasmids (180 ng pGL4 and 20 ng pShuttle/RL) were used for transfection using Lipofectamine 2000 Transfection Reagent (Invitrogen). In MN we used 480 ng pGL4 and 20 ng pShuttle/RL. Two days after DNA transfection, the luciferase activities were measured in Glomax luminometer (Promega) with the Dual-Glo Luciferase Assay System (Promega) according to manufacturer's instructions. One-way ANOVA was performed using GraphPad Prism version 5.00 (San Diego, CA, USA).

Zebrafish animal model

Adult zebrafish were maintained at 28°C on a 14 h light/10 h dark cycle and the embryos were obtained by natural mating. Zebrafish presents only one *klc2* gene in its genome (ZFIN ID: ZDB-GENE-030131-2670), which turns appropriate the use *Danio rerio* as animal model in this study. The use of *Danio rerio* in this study was approved by the Committee on the Ethics of Animal Experiments of Pharmacology and Biochemistry Sciences department of National University of Rosario, Argentina (No. 429/2014).

Zebrafish RNA extraction and cDNA synthesis

Total RNA was extracted from whole embryos at different embryonic stages (6, 24, 48 and 72-hpf). RNA extraction was performed using TRIZOL® reagent (Invitrogen), following the manufacturer's protocol. First-strand cDNA was synthetized using SuperScript Reverse Transcriptase (Invitrogen) with a specific primer (primer ID 3) for *Danio rerio klc2* gene transcript (Ensembl ENSDARG00000075485). The complete *klc2* CDS was amplified by PCR using primers ID 4, forward including *EcoRI* and reverse including *SacI* restriction sites.

Plasmids and DNA constructs

The complete CDS sequence from *klc2* (mRNA^{klc2}) was cloned using *EcoRI* and *SacI* sites into an engineered version of pCS2 +MT as described elsewhere (52). This plasmid was used to

transcribe mRNA$^{klc2\text{-}eGFP}$ coding for KLC2 fused to eGFP. Plasmid without *klc2* insert was used to transcribe mRNA^{eGFP} as a control. For mRNA$^{klc2\text{-}eGFP}$ and mRNA^{eGFP} transcription, plasmids were linearized by *NotI* and the SP6 promoter was used for *in vitro* transcription using mMESSAGE mMACHINE® Kit (Ambion, Applied Biosystems). The mRNA$^{klc2\text{-}eGFP}$ was used to perform the overexpression assay and for rescue of morphant's phenotype.

Knockdown and overexpression assays

Microinjection of morpholino oligonucleotides (MO) in the yolk of embryos at one- to two-cell stage were performed in specific concentrations (4 and 6 ng). Translation blocking morpholino (MO$^{klc2\text{-}TB}$) sequence was 5′-GGTGGACATCACCCACTGACACACA-3′ (misMO$^{klc2\text{-}TB}$ was 5′-GGaGcACATgACCCAgTcACACACA-3′) and splicing blocking morpholino (MO$^{klc2\text{-}SP}$) sequence was 5′-CGTGT GTGTTTCACCTGTGCTTCCC-3′ (misMO$^{klc2\text{-}SP}$ was 5′-CGTcTcT GTTTgACCTcTcCTTCCC-3′). MO$^{klc2\text{-}SP}$ target exon 2 of *klc2* gene. The rescue of phenotype was performed by co-injecting 6 ng MO$^{klc2\text{-}SP}$ and 100 pg mRNA$^{klc2\text{-}eGFP}$ in the yolk of embryos staged at one- to two-cells. Chi-square and Fisher's exact tests were performed using GraphPad Prism version 5.00 (San Diego, CA, USA).

Overxpression of *klc2* gene in zebrafish was performed by microinjecting mRNA$^{klc2\text{-}eGFP}$ at specific concentrations (100, 150 and 200 pg), as described in previous study ([53]). Same concentrations of mRNA^{eGFP} were microinjected in zebrafish embryos to be used as controls. Both microinjected embryos (mRNA$^{klc2\text{-}eGFP}$ and mRNA^{eGFP}) were selected by fluorescence at 24-hpf stage and evaluated at 48-hpf under MVX10 Olympus Microscope, and recorded with MVXTV1XC Olympus digital camera. Chi-square test was performed using GraphPad Prism version 5.00 (San Diego, CA, USA).

Supplementary Material

Supplementary Material is available at *HMG* online.

Acknowledgements

Funding

References

1. Lo Giudice, T., Lombardi, F., Santorelli, F.M., Kawarai, T. and Orlacchio, A. (2014) Hereditary spastic paraplegia: clinical-genetic characteristics and evolving molecular mechanisms. *Exp. Neurol. Nov.*, **261**, 518–539.

2. Macedo-Souza, L., Kok, F., Santos, S., Amorim, S.C., Starling, A., Nishimura, A., Lezirovitz, K., Lino, A.M. and Zatz, M. (2005) Spastic paraplegia, optic atrophy, and neuropathy is linked to chromosome 11q13. *Ann. Neurol.*, **57**, 730–737.

3. Macedo-Souza, L., Kok, F., Santos, S., Licinio, L., Lezirovitz, K., Cavaçana, N., Bueno, C., Amorim, S., Pessoa, A., Graciani, Z. *et al.* (2009) Spastic paraplegia, optic atrophy, and neuropathy: new observations, locus refinement, and exclusion of candidate genes. *Ann. Hum. Genet.*, **73**, 382–387.

4. Windpassinger, C., Auer-Grumbach, M., Irobi, J., Patel, H., Petek, E., Hörl, G., Malli, R., Reed, J.A., Dierick, I., Verpoorten, N. *et al.* (2004) Heterozygous missense mutations in BSCL2 are associated with distal hereditary motor neuropathy and Silver syndrome. *Nat. Genet.*, **36**, 271–276.

5. Novarino, G., Fenstermaker, A.G., Zaki, M.S., Hofree, M., Silhavy, J.L., Heiberg, A.D., Abdellateef, M., Rosti, B., Scott, E., Mansour, L. *et al.* (2014) Exome sequencing links corticospinal motor neuron disease to common neurodegenerative disorders. *Science*, **31**, 506–511.

6. Vale, R.D. (2003) The molecular motor toolbox for intracellular transport. *Cell*, **112**, 467–480.

7. Hirokawa, N., Noda, Y., Tanaka, Y. and Niwa, S. (2009) Kinesin superfamily motor proteins and intracellular transport. *Nat. Rev. Mol. Cell Biol.*, **10**, 682–696.

8. Visscher, K., Schnitzer, M.J. and Block, S.M. (1999) Single kinesin molecules studied with a molecular force clamp. *Nature*, **400**, 184–189.

9. Verhey, K.J. and Hammond, J.W. (2009) Traffic control: regulation of kinesin motors. *Nat. Rev. Mol. Cell Biol.*, **10**, 765–777.

10. Hirokawa, N., Niwa, S. and Tanaka, Y. (2010) Molecular motors in neurons: transport mechanisms and roles in brain function, development, and disease. *Neuron*, **68**, 610–638.

11. Pernigo, S., Lamprecht, A., Steiner, R.A. and Dodding, M.P. (2013) Structural basis for kinesin-1: cargo recognition. *Science*, **340**, 356–359.

12. Rahman, A., Friedman, D.S. and Goldstein, L.S.B. (1998) Two kinesin light chain genes in mice: identification and characterization of the encoded proteins. *J. Biol. Chem.*, **273**, 15395–15403.

13. Perlson, E., Maday, S., Fu, M.M., Moughamian, A.J. and Holzbaur, E.L. (2010) Retrograde axonal transport: pathways to cell death? *Trends Neurosci.*, **33**, 335.

14. Millecamps, S. and Julien, J.P. (2013) Axonal transport deficits and neurodegenerative diseases. *Nat. Rev. Neurosci.*, **14**, 161–176.

15. Reid, E., Kloos, M., Ashley-Koch, A., Hughes, L., Bevan, S., Svenson, I.K., Graham, F.L., Gaskell, P.C., Dearlove, A., Pericak-Vance, M.A. *et al.* (2002) A kinesin heavy chain (KIF5A) mutation in hereditary spastic paraplegia (SPG10). *Am. J. Hum. Genet.*, **71**, 1189–1194.

16. Ebbing, B., Mann, K., Starosta, A., Jaud, J., Schöls, L., Schüle, R. and Woehlke, G. (2008) Effect of spastic paraplegia mutations in KIF5A kinesin on transport activity. *Hum. Mol. Genet.*, **17**, 1245–1252.

17. Caballero Oteyza, A., Battaloğlu, E., Ocek, L., Lindig, T., Reichbauer, J., Rebelo, A.P., Gonzalez, M.A., Zorlu, Y., Ozes, B., Timmann, D. *et al.* (2014) Motor protein mutations cause a new form of hereditary spastic paraplegia. *Neurology*, **3**, 2007–2016.

18. Lee, J., Srour, M., Kim, D., Hamdan, F.F., Lim, S.H., Brunel-Guitton, C., Décarie, J.C., Rossignol, E., Mitchell, G.A., Schreiber, A. *et al.* (2015) De novo mutations in the motor domain of KIF1A cause cognitive impairment, spastic paraparesis, axonal neuropathy and cerebellar atrophy. *Hum. Mutat.*, **36**, 69–78.

19. Munch, C., Rosenbohm, A., Sperfeld, A.D., Uttner, I., Reske, S., Krause, B.J., Sedlmeier, R., Meyer, T., Hanemann, C.O., Stumm, G. *et al.* (2005) Heterozygous R1101K mutation of

the DCTN1 gene in a family with ALS and FTD. *Ann. Neurol.*, **58**, 777.

20. Falzone, T.L., Stokin, G.B., Lillo, C., Rodrigues, E.M., Wester-man, E.L., Williams, D.S. and Goldstein, L.S. (2009) Axonal stress kinase activation and tau misbehavior induced by kinesin-1 transport defects. *J. Neurosci.*, **29**, 5758.

21. Füger, P., Sreekumar, V., Schüle, R., Kern, J.V., Stanchev, D.T., Schneider, C.D., Karle, K.N., Daub, K.J., Siegert, V.K., Flötenmeyer, M. *et al.* (2012) Spastic paraplegia mutation N256S in the neuronal microtubule motor KIF5A disrupts axonal transport in a Drosophila HSP model. *PLoS Genet.*, **8**, e1003066.

22. Valdmanis, P.N., Meijer, I.A., Reynolds, A., Lei, A., MacLeod, P., Schlesinger, D., Zatz, M., Reid, E., Dion, P.A., Drapeau, P. *et al.* (2007) Mutations in the KIAA0196 gene at the SPG8 locus cause hereditary spastic paraplegia. *Am. J. Hum. Genet.*, **80**, 152–161.

23. Lin, P., Li, J., Liu, Q., Mao, F., Li, J., Qiu, R., Hu, H., Song, Y., Yang, Y., Gao, G. *et al.* (2008) A missense mutation in SLC33A1, which encodes the acetyl-CoA transporter, causes auto-somal-dominant spastic paraplegia (SPG42). *Am. J. Hum. Genet.*, **83**, 752–759.

24. Clemen, C.S., Tangavelou, K., Strucksberg, K.H., Just, S., Gaertner, L., Regus-Leidig, H., Stumpf, M., Reimann, J., Coras, R., Morgan, R.O. *et al.* (2010) Strumpellin is a novel valosin-containing protein binding partner linking heredi-tary spastic paraplegia to protein aggregation diseases. *Brain*, **133**, 2920–2941.

25. Fassier, C., Hutt, J.A., Scholpp, S., Lumsden, A., Giros, B., Nothias, F., Schneider-Maunoury, S., Houart, C. and Hazan, J. (2010) Zebrafish atlastin controls motility and spinal motor axon architecture via inhibition of the BMP pathway. *Nat. Neurosci.*, **13**, 1380–1387.

26. Martin, E., Yanicostas, C., Rastetter, A., Naini, S.M., Maouedj, A., Kabashi, E., Rivaud-Péchoux, S., Brice, A., Stevanin, G. and Soussi-Yanicostas, N. (2012) Spatacsin and spastizin act in the same pathway required for proper spinal motor neuron axon outgrowth in zebrafish. *Neurobiol. Dis.*, **48**, 299–308.

27. Martin, E., Schüle, R., Smets, K., Rastetter, A., Boukhris, A., Loureiro, J.L., Gonzalez, M.A., Mundwiller, E., Deconinck, T., Wessner, M. *et al.* (2013) Loss of function of glucocerebrosi-dase GBA2 is responsible for motor neuron defects in heredi-tary spastic paraplegia. *Am. J. Hum. Genet.*, **92**, 238–244.

28. Song, Y., Wang, M., Mao, F., Shao, M., Zhao, B., Song, Z., Shao, C. and Gong, Y. (2013) Knockdown of Pnpla6 protein results in motor neuron defects in zebrafish. *Dis. Model Mech.*, **6**, 404–413.

29. Cremers, F.P.M., Pfeiffer, R.A., van de Pol, T.J., Hofker, M.H., Kruse, T.A., Wieringa, B. and Ropers, H.H. (1987) An intersti-tial duplication of the X chromosome in a male allows phys-ical fine mapping of probes from the Xq13-q22 region. *Hum. Genet.*, **77**, 23–27.

30. Hodes, M.E., Pratt, V.M. and Dlouhy, S.R. (1993) Genetics of Pelizaeus-Merzbacher disease. *Dev. Neurosci.*, **15**, 383–394.

31. Inoue, K., Osaka, H., Sugiyama, N., Kawanishi, C., Onishi, H., Nezu, A., Kimura, K., Yamada, Y. and Kosaka, K. (1996) A duplicated PLP gene causing Pelizaeus-Merzbacher disease detected by comparative multiplex PCR. *Am. J. Hum. Genet.*, **59**, 32–39.

32. Mimault, C., Giraud, G., Courtois, V., Cailloux, F., Boire, J.Y., Dastugue, B. and Boespflug-Tanguy, O. (1999) Clinical European network on brain dysmyelinating disease. Proteoli-poprotein gene analysis in 82 patients with sporadic Peli-zaeus-Merzbacher disease: duplications, the major cause of

the disease, originate more frequently in male germ cells, but point mutations do not. *Am. J. Hum. Genet.*, **65**, 360–369.

33. Carvalho, C.M.B., Ramocki, M.B., Pehlivan, D., Franco, L.M., Gonzaga-Jauregui, C., Fang, P., McCall, A., Pivnick, E.K., Hines-Dowell, S., Seaver, L.H. *et al.* (2011) Inverted genomic segments and complex triplication rearrangements are mediated by inverted repeats in the human genome. *Nat. Genet.*, **43**, 1074–1081.

34. Hertz, J.M., Borglum, A.D., Brandt, C.A., Flint, T. and Bisgaard, C. (1994) Charcot-Marie-Tooth disease type 1A: the parental origin of a de novo 17p11.2-p12 duplication. *Clin. Genet.*, **46**, 291–294.

35. Sorour, E., Thompson, P., MacMillan, J. and Upadhyaya, M. (1995) Inheritance of CMT1A duplication from a mosaic father. *J. Med. Genet.*, **32**, 483–485.

36. Theuns, J., Brouwers, N., Engelborghs, S., Sleegers, K., Bogaerts, V., Corsmit, E., De Pooter, T., van Duijn, C.M., De Deyn, P.P. and Van Broeckhoven, C. (2006) Promoter mutations that increase amyloid precursor-protein expres-sion are associated with Alzheimer disease. *Am. J. Hum. Genet.*, **78**, 936–946.

37. Nagaraj, K., Kristiansen, L.V., Skrzynski, A., Castiella, C., Garcia-Alonso, L. and Hortsch, M. (2009) Pathogenic human L1-CAM mutations reduce the adhesion-dependent activation of EGFR. *Hum. Mol. Genet.*, **18**, 3822–3831.

38. Meijer, I.A., Dion, P., Laurent, S., Dupré, N., Brais, B., Levert, A., Puymirat, J., Rioux, M.F., Sylvain, M., Zhu, P.P. *et al.* (2007) Characterization of a novel SPG3A deletion in a French-Can-adian family. *Ann. Neurol.*, **61**, 599–603.

39. Havlicek, S., Kohl, Z., Mishra, H.K., Prots, I., Eberhardt, E., Den-guir, N., Wend, H., Plötz, S., Boyer, L., Marchetto, M.C. *et al.* (2014) Gene dosage-dependent rescue of HSP neurite defects in SPG4 patients' neurons. *Hum. Mol. Genet.*, **15**, 2527–2541.

40. Bakowska, J.C., Wang, H., Xin, B., Sumner, C.J. and Blackstone, C. (2008) Lack of spartin protein in Troyer syndrome: a loss-of-function disease mechanism? *Arch. Neurol.*, **65**, 520–524.

41. Kruer, M.C., Paisán-Ruiz, C., Boddaert, N., Yoon, M.Y., Hama, H., Gregory, A., Malandrini, A., Woltjer, R.L., Munnich, A., Gobin, S. *et al.* (2010) Defective FA2H leads to a novel form of neurodegeneration with brain iron accumulation (NBIA). *Ann. Neurol.*, **68**, 611–618.

42. Li, H. and Durbin, R. (2010) Fast and accurate long-read align-ment with Burrows-Wheeler transform. *Bioinformatics*, **26**, 589–595.

43. McKenna, A., Hanna, M., Banks, E., Sivachenko, A., Cibulskis, K., Kernytsky, A., Garimella, K., Altshuler, D., Gabriel, S., Daly, M. *et al.* (2010) The Genome Analysis Toolkit: a MapReduce framework for analyzing next-generation DNA sequencing data. *Genome Res.*, **20**, 1297–1303.

44. Wang, K., Li, M. and Hakonarson, H. (2010) ANNOVAR: Func-tional annotation of genetic variants from next-generation sequencing data. *Nucleic Acids Res.*, **38**, e164.

45. Plagnol, V., Curtis, J., Epstein, M., Mok, K.Y., Stebbings, E., Gri-goriadou, S., Wood, N.W., Hambleton, S., Burns, S.O., Thrash-er, A.J. *et al.* (2012) A robust model for read count data in exome sequencing experiments and implications for copy number variant calling. *Bioinformatics*, **28**, 2747–2754.

46. Cingolani, P., Platts, A., Wang le, L., Coon, M., Nguyen, T., Wang, L., Land, S.J., Lu, X. and Ruden, D.M. (2012) A program for annotating and predicting the effects of single nucleotide polymorphisms, SnpEff: SNPs in the genome of Drosophila melanogaster strain w1118; iso-2; iso-3. *Fly*, **6**, 80–92.

47. Marchetto, M.C., Carromeu, C., Acab, A., Yu, D., Yeo, G.W., Mu, Y., Chen, G., Gage, F.H. and Muotri, A.R. (2010) A model for

neural development and treatment of Rett syndrome using human induced pluripotent stem cells. *Cell*, **12**, 527–539.

48. Mitne-Neto, M., Machado-Costa, M., Marchetto, M.C., Bengtson, M.H., Joazeiro, C.A., Tsuda, H., Bellen, H.J., Silva, H.C., Oliveira, A.S., Lazar, M. *et al.* (2011) Downregulation of VAPB expression in motor neurons derived from induced pluripotent stem cells of ALS8 patients. *Hum. Mol. Genet.*, **15**, 3642–3652.

49. Irizarry, R.A., Hobbs, B., Collin, F., Beazer-Barclay, Y.D., Antonellis, K.J., Scherf, U. and Speed, T.P. (2003) Exploration, normalization, and summaries of high density oligonucleotide array probe level data. *Biostatistics*, **4**, 249–264.

50. Schmittgen, T.D. and Livak, K.J. (2008) Analyzing real-time PCR data by the comparative C(T) method. *Nat. Protoc.*, **3**, 1101–1108.

51. Soltys, D.T., Rocha, C.R., Lerner, L.K., de Souza, T.A., Munford, V., Cabral, F., Nardo, T., Stefanini, M., Sarasin, A., Cabral-Neto, J.B. *et al.* (2013) Novel XPG (ERCC5) mutations affect DNA repair and cell survival after ultraviolet but not oxidative stress. *Hum. Mutat.*, **34**, 481–489.

52. Favaro, F.P., Alvizi, L., Zechi-Ceide, R.M., Bertola, D., Felix, T.M., de Souza, J., Raskin, S., Twigg, S.R., Weiner, A.M., Armas, P. *et al.* (2014) A noncoding expansion in EIF4A3 causes Richieri-Costa-Pereira syndrome, a craniofacial disorder associated with limb defects. *Am. J. Hum. Genet.*, **94**, 120–128.

53. Niederriter, A., Davis, E.E., Golzio, C., Oh, E.C., Tsai, I.C. and Katsanis, N. (2013) In vivo modeling of the morbid human genome using Danio rerio. *J. Vis. Exp.*, **24**, e50338.